Available online at www.sciencedirect.com
SCIENCE DIRECT
Scripta Materialia 54 (2006) 741–746
Scripta MATERIALIA
www.actamat-journals.com

Physical analyses of crystal plasticity by DD simulations

B. Devincre [a,*], L. Kubin [a], T. Hoc [b]

[a] Laboratoire d'Etude des Microstructure, UMR104, CNRS-ONERA, 29 Av. de la Division Leclerc, 92322 Chatillon Cedex, France
[b] Laboratoire MSSMat, UMR 8570 CNRS, Ecole Centrale Paris, Grande Voie des Vignes, 92295 Chatenay-Malabry Cedex, France

Received 29 August 2005; received in revised form 19 October 2005; accepted 26 October 2005
Available online 23 November 2005

Abstract

The present work emphasises the potentialities of dislocation dynamics simulations for performing analyses of crystal plasticity and obtaining information that cannot be reached by experiment. As an example, a study is presented of parameters that are critical for modeling strain hardening in face-centred cubic crystals, the mesoscopic coefficients of interaction between non-coplanar slip systems.

Keywords: Plastic deformation; Dislocation dynamics; Strain hardening; Simulation; Forest interactions

1. Introduction

Three-dimensional dislocation dynamics (DD) simulations now have a rather wide domain of application. In particular, these mesoscale simulations are of interest for addressing in a predictive manner the complex problems of dislocation patterning and strain hardening in crystals. From the beginning of dislocation theory, these questions were identified as the first step towards the building up of a physically-based theory of plastic flow.

The plastic properties of face-centred cubic (fcc) crystals are experimentally well documented. They depend on elastic properties of dislocations and, at low and medium temperatures, on only one important core mechanism, cross-slip. This makes fcc crystals the best possible model materials for carrying out fundamental studies by DD simulations. In what follows, this approach is discussed and exemplified through the determination of a few critical parameters involved in strain hardening models. Specifically, the present work deals with model simulations of the interaction between dislocations gliding in non-coplanar slip systems and on the integration of the results in a form suited for dislocation-based modeling.

2. Forest hardening in fcc crystals

This section briefly outlines a few facts about dislocation hardening, that is the relation between flow stress and dislocation densities, as well as recent contributions from DD simulations, which are relevant to the present investigation. The flow stress, τ, follows the classical Taylor relation, $\tau = \alpha\mu b\sqrt{\rho_f}$, where μ is the shear modulus, b the magnitude of the Burgers vector, ρ_f the forest (i.e. intersecting) dislocation density and $\alpha \approx 0.35 \pm 0.1$.

It was understood rather early on that short-range reactions between dislocations, when present, are responsible for most of the flow stress [1]. As a consequence, many studies have focused on the rather complicated task of estimating the strength of specific dislocation reactions, using a simplified elastic framework, and further deriving the collective strength of the forest, α, by performing an average over the spectrum of strengths associated with all possible configurations [1,2]. It was further realised that DD simulations represent an ideal tool for performing difficult elastic computations and complex global averages. They also have the advantage of accounting for short-range interactions, including crossed-states, that is attractive

* Corresponding author. Tel.: +33 1 46 73 44 49; fax: +33 1 46 73 41 55.
E-mail addresses: benoit.devincre@onera.fr, devincre@onera.fr (B. Devincre).

1359-6462/$ - see front matter
doi:10.1016/j.scriptamat.2005.10.066

intersections that do not form junctions [3], as well as long-range interactions.

Two main conclusions emerged from such mesoscale simulations. In agreement with earlier predictions, the flow stress is found to be rather insensitive to long-range elastic interactions in multislip conditions. It is mostly controlled by junction formation and destruction [4]. In conditions of monotonic straining, comparisons were performed between simulated configurations exhibiting dislocation self-organization in the presence of cross-slip and rather uniform dislocation distributions in the absence of cross-slip [5]. It is usually assumed that cross-slip processes favour the formation of three-dimensional patterns by relaxing the conditions of purely planar glide that would prevail in its absence. Nevertheless, the flow stress practically does not depend on the cross-slip activity and on the organization of the dislocation microstructure. This relative insensitivity of the flow stress to dislocation patterning explains why the Taylor equation is experimentally found to be very robust.

The predictive ability of the Taylor relation is, however, limited since it lumps all densities into a single variable and does not account for the different strengths arising from the pair interactions between possible slip systems. For this reason, the following matrix form of the Taylor equation was proposed by Franciosi [6]:

$$\tau_c^s = \mu b \sqrt{\sum_u a^{su} \rho^u}. \tag{1}$$

In this formulation, the total density is split into a sum of dislocation densities in each slip system, (u), weighted by the strength of the corresponding interactions. The interaction coefficients a^{su} represent the average strength of the mutual interactions between slip systems (s) and (u). All interactions are considered, that is junction-forming interactions, as well as those producing dipoles. The number of distinct interaction coefficients between the 12 mutually interacting slip systems in the fcc structure is reduced to only six for symmetry reasons. Details about the form of the interaction matrix and the specific type of interaction between each pair of slip systems can be found in [7,8]. Little is known experimentally about the values of these interaction coefficients. Only indirect and approximate estimates can be obtained through latent hardening tests on single crystals [6,9,10].

In current models for strain hardening, which are expressed in tensor form (see e.g. [11]), Eq. (1), is considered as yielding the critical stress for the onset of slip in system (s). It is complemented by an expression giving the dependence of the strain rate on the flow stress and by evolutionary laws for the densities in each slip system. These evolutionary laws account for two mechanisms, storage and recovery [12]. The recovery process is related to the annihilation of screw dislocations by cross-slip. It represents the only core mechanism that is not directly accessible to DD simulations in fcc crystals. Dislocation storage describes the pinning of dislocations after a certain mean free path, which is expected to be inversely proportional to the strength of obstacles. It follows that the interaction coefficients are intimately related to the mean free paths of dislocations, a question that is not further developed here due to lack of space. Thus, a measure of the interaction coefficients yields critical parameters for implementing physical models for strain hardening in single crystals.

Four interaction coefficients are of interest in the present study. They are related to the three types of junctions classically described in fcc crystals, viz. the Hirth lock, the glissile junction and the Lomer lock. A fourth interaction is concerned with the collinear reaction, which is the interaction of a slip system with its cross-slip system. As the two systems have same Burgers vector, annihilations of dislocations occur within an extended range of characters. In a preliminary attempt, a set of interaction coefficients was deduced from DD simulations whereby the interaction coefficients for junction-forming configurations were measured one by one [13]. In a further attempt [7], systematic simulations were performed using periodic boundary conditions (PBCs). This last study revealed the very high strength of the collinear reaction, which had not been noticed till then. The results that are presented below respond to two motivations. One derives from the present lack of information on the collective processes governing forest interactions. The second one responds to the need for reasonably accurate values of the interaction coefficients, in order to further develop models that can predict the number and nature of active slip systems and the resulting strain hardening.

3. Model simulations: Methodology

The method used in the present work derives from the one used by Madec et al. [7], which was reformulated to obtain a better precision through an improved control of all possible sources of inaccuracies.

The DD simulation used in the present work is described in [14,15]. Thus, only the specific conditions for model simulations are discussed here. A primary slip system (p) is defined, $\frac{1}{2}[0\,1\,1](1\,1\,\bar{1})$, which is the same in all simulations. The primary dislocations glide through a prescribed density ρ_f of forest dislocations. The latter is made up of a random distribution of dislocations segments of length $2\rho_f^{-1/2}$, with a random distribution of characters. The forest segments are such that their interaction with the primary system produces a single type of reaction. As shown in Table 1, these segments belong to one or two different slip systems, depending upon the interaction considered.

Table 1
The four types of reactions and forest slip systems leading to these reactions by interaction with the primary system $\frac{1}{2}[0\,1\,1](1\,1\,\bar{1})$

Hirth	Glissile	Lomer	Collinear
$\frac{1}{2}[0\,1\,\bar{1}](1\,1\,1)$	$\frac{1}{2}[\bar{1}\,0\,1](1\,\bar{1}\,1)$	$\frac{1}{2}[\bar{1}\,0\,1](1\,1\,1)$	$\frac{1}{2}[0\,1\,1](1\,\bar{1}\,1)$
$\frac{1}{2}[0\,1\,\bar{1}](\bar{1}\,1\,1)$	$\frac{1}{2}[\bar{1}\,1\,0](1\,1\,1)$	$\frac{1}{2}[1\,1\,0](\bar{1}\,1\,1)$	

The simulation cell has a linear dimension of about $10\rho_f^{-1/2}$ and use is made of PBCs. Three forest densities are tested for each interaction, $\rho_f = 10^{11}$, 10^{12} and $10^{13}\,m^{-2}$. A constant plastic strain rate is applied, which must be kept low enough to avoid dynamical effects arising from too large free-flight dislocation velocities. The imposed strain rates are determined by a scaling with respect to the cell dimensions and are 0.1, 4, and $40\,s^{-1}$, respectively, for the three forest densities given above.

The projection of the applied stress on the forest systems is set to zero in order to prevent dislocation multiplication. Thus, ρ_f stays constant during a simulation. This procedure also prevents forest segments from mutually reacting, which would produce undesired obstacles to the motion of primary dislocations. The initial primary density is $\rho_p = \rho_f/5$ and is made up of 20 dislocation lines of length $10\rho_f^{-1/2}$. The cross-slip probability is set to zero, to avoid spurious interactions via the local activation of cross-slip systems. A procedure was also devised to eliminate dipolar interactions at short-distances between dislocations of the primary system. Hence, care was taken to ensure that only one type of interaction is occurring in each model simulation.

Upon loading, and after a transient, the simulated flow stress saturates. The interaction coefficient under investigation can then be determined from Eq. (1) through the knowledge of the steady-state stress and the constant forest density. It was checked that the results obtained do not depend on the value of the initial primary density or the prescribed strain rate. The isotropic elastic constants used are those of copper, but the interaction coefficients being dimensionless material parameters, their values are valid for all fcc crystals.

4. Results

In what follows, a few results are selected, which illustrate the interest of DD simulations for implementing dislocation mechanisms in continuum models. The steady-state configurations yielded by the model simulations are illustrated by Fig. 1 for the four types of reactions. Visual inspection shows that the three junction-forming reactions result in rather similar types of dislocation arrangements and distributions of junction lengths. However, the density of junctions along the primary lines is clearly larger for the glissile and Lomer interactions (Fig. 1a and b) than for the Hirth interactions (Fig. 1c). As all available estimates suggest that the Hirth lock is the weakest of all junctions, this indicates that the strength of interactions depends on both the length and number of junctions. Both quantities are related to the length of the neighbouring primary arms. The lengths of the latter then govern the unzipping process by which the junctions are destroyed. This is manifested by the rather large curvature radii associated of segments connected by Hirth locks, as compared with the two other types of junctions.

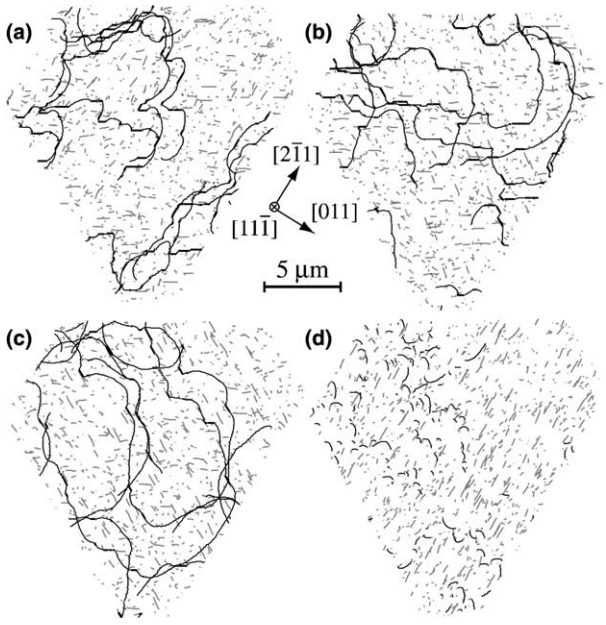

Fig. 1. Thin foils of thickness 0.5 μm extracted from model simulations of the interaction strength between slip systems. The forest density is $\rho_f = 10^{12}\,m^{-2}$ and the foil plane is the primary slip plane. The imposed plastic strain rate is $4\,s^{-1}$. (a), (b), (c) and (d) correspond to the glissile, Lomer, Hirth and collinear reactions, respectively. The initial configuration in the primary slip system $\frac{1}{2}[0\,1\,1](1\,1\,\bar{1})$ is the same in all cases. Forest segments appear in grey, primary lines in black and junctions as straight, thick black lines.

The dynamic sequences[1] show that the mobile primary dislocations propagate through the forest through successions of unpinning bursts. The unzipping of a junction induces a cascade of secondary unzipping events along the primary line, which propagates sideways until new stable junctions are formed. For the collinear interaction (Fig. 1d), the configuration and the dynamic behavior are very specific. The collinear annihilations result in the formation of a number of small segments. These segments bow out under stress until a critical configuration is reached for their remobilisation. The very small curvature radii in Fig. 1d, attests the very high strength of this interaction. Thus, the hierarchy of reaction strengths obtained in a previous study [7] can be directly visualised from Fig. 1.

To quantify the primary microstructure, the distributions of junction lengths were first examined. This allows, in addition, a comparison to be performed with the more realistic distributions obtained from 3D "mass simulations" in multislip conditions with [0 0 1] and [1 1 1] stress axes. In this last case, the length and spatial distributions of the forest dislocations are not imposed, whereas in the model simulations all forest segments have same length, are distributed at random and cannot move over large

[1] These sequences can be viewed at <http://zig.onera.fr/DisGallery/coef.html>.

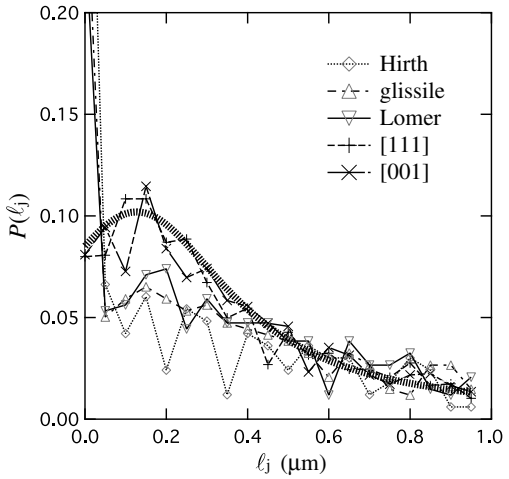

Fig. 2. Plots of the probability $P(\ell_j)$ for finding a junction of length ℓ_j under stress, for a forest density, $\rho_f = 10^{12}\,m^{-2}$. Empty symbols correspond to model simulations. Others symbols refer to mass simulations of tensile tests along [0 0 1] and [1 1 1] orientations. The dashed line is a fit of these last two distributions that serves as a guide to the eye. The length 1 μm represents the average segment length, $\rho_f^{-1/2}$.

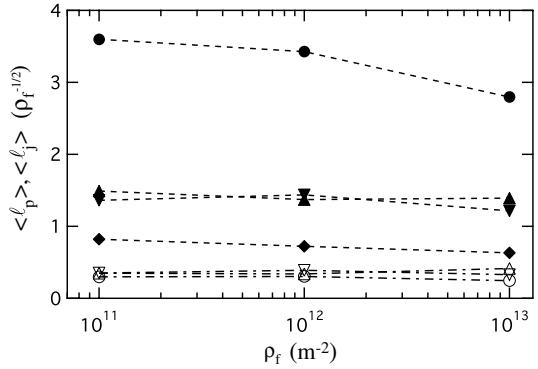

Fig. 3. Plots of the mean junction lengths, $\langle \ell_j \rangle$ and primary segment lengths, $\langle \ell_p \rangle$, vs. the forest density. ○, △ and ▽: average junction length for the Hirth, glissile and Lomer reactions, respectively. ●, ▲, ▼ and ♦: average length of the primary segments for the Hirth, glissile, Lomer and collinear interactions, respectively.

Table 2
Interaction coefficient values for the four types of reactions between slip systems in fcc crystals

a_{ortho} (Hirth)	a_2 (glissile)	a_3 (Lomer)	a_{coli} (collinear)
0.0454 ± 0.003	0.137 ± 0.014	0.122 ± 0.012	0.625 ± 0.044

The coefficients are designated according to their traditional nomenclature and the corresponding type of interaction. These values are given for a reference value of the forest density, $\rho_f = 10^{12}\,m^{-2}$.

distances. The probabilities $P(\ell_j)$ for finding junctions of length ℓ_j under stress are shown in Fig. 2.

The histograms obtained from mass simulations exhibit a generic shape looking like a truncated pseudo-Gaussian distribution, with a well-defined maximum and a smoothly decreasing tail. The non-zero probability for $\ell_j = 0$ reflects the occurrence of crossed-states, that is junctions of null length. The model simulations yield comparable distributions, especially for the largest junction lengths. The position of the maximum probability, at $0.15\rho_f^{-1/2}$, is well reproduced. This results from the value adopted for the length of the forest segments, $2\rho_f^{-1/2}$. The distributions yielded by model simulations appear to have a deficit in the number of junction lengths around the maximum, and an excess of very small junctions lengths and crossed-states. This last feature may be attributed to the uniform distribution of characters in the forest density, as the more complex interactions occurring in mass simulations should favour some redistribution of the local orientations. This difference is assumed not to affect the measurement of the interaction coefficients because, in statistical terms, short junctions and crossed-states are connected to long unzipping arms. The flow stress is mostly determined by long junction segments, which are on average connected to small arms and require large unzipping stresses.

The mean values of the junction lengths and of the lengths of the primary segments are plotted as a function of the forest density in Fig. 3. The average lengths of the primary segments, $\langle \ell_p \rangle$ scale with $\rho_f^{-1/2}$ (in an approximate manner for the Hirth lock) and depend on the type of interaction considered. This confirms a trend suggested above, specifically that the interaction strengths essentially depend on the length of the unzipping arms. The Hirth lock is the weakest junction because it has the largest value of $\langle \ell_p \rangle$. Conversely, the collinear interaction is the strongest because it is associated with the smallest value of $\langle \ell_p \rangle$ (Fig. 3). Assuming, then, that $\langle \ell_p \rangle \propto 1/\sqrt{a\rho_f}$, Eq. (1) yields, for a single type of interaction, $\tau_a \propto \mu b/\langle \ell_p \rangle$. One can check from the values of the interaction coefficients presented in Table 2 that this expression is well verified.

In addition, Fig. 3 reveals an intriguing feature. The average value of the junction lengths, $\langle \ell_j \rangle$, also scales with $\rho_f^{-1/2}$. More precisely, we find $\langle \ell_j \rangle \approx 0.25\rho_f^{-1/2}$, irrespective of the type of junction and the average length of the parent primary segments, $\langle \ell_p \rangle$. A similar property is yielded by the distributions shown in Fig. 2, wherein all the maxima seem to occur at the same position, $\ell_j \approx 0.15\rho_f^{-1/2}$. This seems to confirm that the scaled distribution of junction lengths under stress can be approximated by an universal distribution, with fixed positions for the maximum and the average value.

The interaction coefficients are obtained from the steady-state flow stress τ in the form $\tau\rho_f^{-1/2}/\mu b$ and plotted as a function of $\rho_f^{-1/2}$ in Fig. 4. It clearly appears from this figure that the four interaction coefficients are not constant and drift toward larger values when $\rho_f^{-1/2}$ increases. This observation parallels a similar result obtained in mass simulations of the tensile deformation of [0 0 1] crystals [4]. The coefficient α involved in the scalar Taylor relation was also found to drift in the same manner as the present interaction coefficients. The reason for this effect is actually known from earlier studies [2,9]. In its conventional form, the

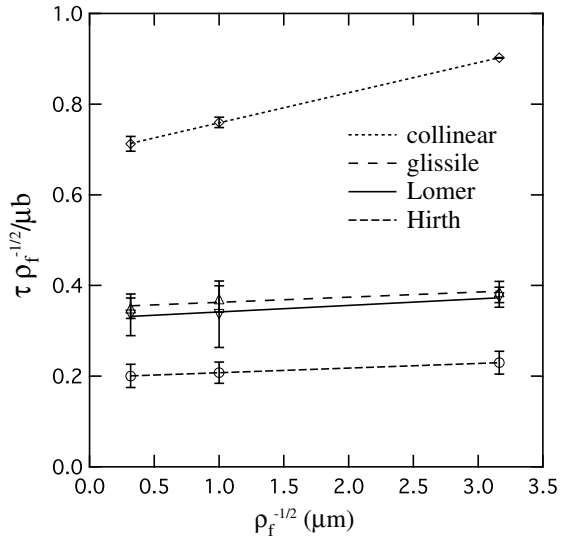

Fig. 4. Values of the interaction coefficients in the form yielded by the expanded Taylor equation (Eq. (1)), as a function of the forest density for the four types of reactions between slip systems. The error bars mainly reflect the stress fluctuations resulting from unpinning bursts. Linear regression lines are drawn through each data set.

Taylor relation makes use of a simplified expression of the line tension, $T \approx \mu b^2$. Fig. 4 shows without ambiguity that this simplified form is not adequate and suggests adopting a more accurate form of the line tension, which accounts for its logarithmic dependence on two cut-off radii. As the primary dislocations bow out under stress, all the more as the interaction strength is significant, this suggests taking the outer cut-off radius in the form $R = \langle \ell_p \rangle \approx 1/\sqrt{a\rho_f}$. Adopting a reference value $\rho_{ref} = 10^{12}\,m^{-2}$ for the forest density, the modified Eq. (1) for a single type of interaction reads:

$$\tau_c^s = \mu b \frac{\ln(1/b\sqrt{a\rho_f})}{\ln(1/b\sqrt{a\rho_{ref}})}\sqrt{a\rho_f}, \qquad (2)$$

where b represents the lower cut-off radius. Each interaction coefficient then becomes weakly dependent on the forest density and its reference value is defined from the reference value of the forest density. Eq. (2) was solved numerically for each interaction, using separately the data sets obtained for each forest density. The results yield a very good fit of the plots of Fig. 4, all the more as the results from DD simulations are redundant (three equation and two unknowns per interaction). The reference values for the interaction coefficients are reproduced in Table 2, using a nomenclature due to Franciosi [6].

Before commenting on these values, the case of the glissile interaction has to be discussed. Glissile junctions may bow out critically in the primary or the secondary slip system. Thus, their strength may depend on the mode of loading and on the Schmid factor in the two slip planes. For instance, one can see from Table 1 that the interaction of primary dislocations with the forest system $\frac{1}{2}[\bar{1}\,1\,0](1\,1\,1)$ leads to the formation of glissile junctions of Burgers vector $\frac{1}{2}[1\,0\,1]$. Upon loading along any orientation like $[\bar{1}, k, 1]$, with k arbitrary, the Schmid factor is zero on the glissile junctions and they cannot bow out. In the present work, all junctions were assumed to be sessile for the sake of simplicity. This may lead to an overestimated value for the coefficient a_2, when the loading is such that glissile junctions can bow out critically before being unzipped. This probability is, however, unlikely to be very significant since the average length of glissile junctions $\langle \ell_j \rangle$ is six times smaller than the average length $\langle \ell_p \rangle$ of the unzipping arms (Fig. 3). Thus, there is in principle, no way to define a universal value for the strength of the glissile junction. Considering the results shown in Table 2 and the numerical uncertainties, one may assume for modeling purposes that the coefficients corresponding to the glissile junction and the Lomer lock are always of comparable strength.

The Hirth lock is definitely the weakest of all junctions and the collinear interaction is the strongest. As discussed in [16,17], one among several important consequences of this strength is that two slip systems interacting by the collinear interaction cannot be simultaneously activated. As a result, the glissile and Lomer interactions control the flow stress in most cases of multislip conditions. This can be checked from the values of $a_2^{1/2}$ and $a_3^{1/2}$, respectively 0.37 and 0.35, which are consistent with the value $\alpha \approx 0.35$ in the scalar Taylor relation.

5. Concluding remarks

Unpublished ongoing studies on single crystal plasticity show that the coefficients of interaction strength between slip systems must be determined with a reasonably good accuracy to obtain a correct prediction of the activated slip systems for all crystal orientations. For this reason, extreme care has been taken in the present work to eliminate all sources of errors and artefacts. The final set of values presented here confirms the qualitative trends previously obtained and provides a set of values that are sufficiently accurate for modeling purposes. The two coefficients corresponding to dipolar interactions, the self-interaction and the coplanar interaction, are not considered here because they deserve a separate discussion (see [18] for the self-interaction).

The measurement of interaction strengths between slip systems allows removing a number of free parameters from crystal plasticity models. Indeed, these coefficients govern the critical stress for slip system activity and are also involved in the definition of the dislocation mean free paths. Thus, the outcome of DD simulations contributes here to attributing a predictive character to "metallurgical" models for strain hardening, by estimating the values of all the coefficients that describe elastic interactions. These models contain more physics than is usually assumed. For instance, Taylor-type equations can be split into a small contribution for long-range interactions and a large one for short-range interactions. This last part represents an average over an extremely complex local spectrum of

discrete junction configurations. It can, therefore, be seen as a result of a coarse-graining that is performed by DD simulations in a volume that is representative of the bulk single crystal.

A model for strain hardening in single crystals is now within reach for the first time, after nearly fifty years of efforts, which can be further applied to polycrystals and materials with more complex microstructures. The advantages of this type of model are that they are rather simple and can be directly compared to experiment. They also benefit from the relative insensitivity of the mechanical response to the spatial organization of the dislocation microstructure during monotonic deformation, a feature that certainly deserves more discussion.

Such models, which incorporate a single, uniform density, reach their limits in two situations where the spatial organization of dislocations does matter. One seems to be met at very large strains, typically somewhere near the end of stage III, and the other is found when a change in strain path is imposed. This is for instance the case in Bauschinger tests, where the sign of the applied strain rate is abruptly changed during plastic flow. A fraction of the immobilized dislocation density is then remobilized and moves back. The modeling of this feature obviously requires a description of the dislocation microstructure. The next modeling step implies that some connection be established at some point with stochastic models for patterning (see Zaiser, this issue), or the more ambitious and much more complex, statistical models that are currently under development. It is worth noting at this point that neither DD simulations, nor continuum models, can at present incorporate dislocation core properties without making simplifying assumptions.

Statistical models mark a revival of the traditional continuum theory and attempt at redeeming its three major shortcomings, namely its static character, the definition of a characteristic distance for coarse-graining the dislocation densities within an evolving microstructure and the incorporation of short-range discrete dislocation mechanisms and interactions. Statistical models focus, inter alia, on the continuous description of the dislocation lines, on stress equilibrium and other conditions imposed by the continuum theory, on the derivation of the kinetics of dislocation motion from statistical mechanics considerations, and on the treatment of long-range elastic interactions. Most of them are two-dimensional and may be seen as simplified benchmark tests. Very few are three-dimensional and attempt incorporating dislocation mechanisms that could at some point lead to the formation of realistic patterns (see El-Azab, this issue). Finally, statistical models entail a considerable complexity and no solution has been obtained to date that could be compared to experiment.

Prospectively, and without getting into detail because of feasibility problems, one can imagine several types of cross-checks by which three-dimensional DD simulations could contribute to the development of statistical models. These simulations can be used in the form of mass simulations, as well as model simulations, like the ones presented here, or by switching on and off various features in order to isolate their contribution. In the same manner, specific parts of the statistical models may be tested separately against their counterpart in DD simulations. Another objective could be to validate simplifying assumptions which would make models easier to handle without loss of accuracy. In the case of fcc crystals the problems of concern are, for instance, all kinetic aspects, the consistency of the coarse-graining processes, and the description of contact reactions between dislocation lines.

References

[1] Saada G. Acta Metall 1960;8:841–7.
[2] Schoeck G, Frydman R. Phys Stat Sol (b) 1972;53:661–73.
[3] Wickham LK, Schwarz KW, Stölken JS. Phys Rev Lett 1999;83:4574–7.
[4] Madec R, Devincre B, Kubin L. Phys Rev Lett 2002;89:255508 (1–4).
[5] Madec R, Devincre B, Kubin L. Scr Mater 2002;47:689–95.
[6] Franciosi P, Berveiller M, Zaoui A. Acta Metall 1980;28:273–83.
[7] Madec R, Devincre B, Kubin L, Hoc T, Rodney D. Science 2003;301:1879–82.
[8] Kubin L, Madec R, Devincre B. In: Zbib H, Lassila D, Levine L, Hemker K, editors. Multiscale phenomena in materials—Experiments and modeling related to mechanical behavior. Mater Res Soc Symp Proc, vol. 779. Warrendale, Pennsylvania: MRS; 2003. p. W1.6.
[9] Basinski SJ, Basinski ZS. In: Nabarro FRN, editor. Dislocations in solids, vol. 4. Amsterdam: North Holland; 1979. p. 261–362.
[10] Wu T-Y, Bassani J, Laird C. Proc Roy Soc Lond A 1991;435:1–19.
[11] Teodosiu C, Raphanel JL, Tabourot L. In: Teodosiu C, Raphanel JL, Sidoroff F, editors. Large plastic deformations. Rotterdam: A.A. Balkema; 1993. p. 153–75.
[12] Kocks UF, Mecking H. Prog Mater Sci 2003;48:171–273.
[13] Fivel M, Tabourot L, Rauch E, Canova GR. J Phys IV 1998;8:151–8.
[14] Devincre B, Kubin LP, Lemarchand C, Madec R. Mater Sci Eng A 2001;309–310:211–9.
[15] Monnet G, Devincre B, Kubin L. Acta Mater 2004;52:4317–28.
[16] Madec R, Devincre B, Kubin L. In: Kitagawa H, Shibutani Y, editors. IUTAM symposium on mesoscopic dynamics of fracture process and materials strength. Solid mechanics and its applications, vol. 115. NL-Dordrecht: Kluwer Academic Publishers; 2004. p. 35–44.
[17] Devincre B, Hoc T, Kubin L. Mater Sci Eng A 2005;400–401:182–5.
[18] Hoc T, Devincre B, Kubin L. In: Gundlach C et al., editors. Evolution of deformation microstructures in 3D, Risoe 25th Int Symposium. Risoe Natl. Lab., Denmark, 2004. p. 43–59.